Biogeosciences Discuss., 8, 10187–10227, 2011
www.biogeosciences-discuss.net/8/10187/2011/
doi:10.5194/bgd-8-10187-2011

Biogeosciences Discussions

A model study of the seasonal and long term North Atlantic surface pCO_2 variability

J. F. Tjiputra[1,2], A. Olsen[2,3], K. Assmann[4], B. Pfeil[1,2,5], and C. Heinze[1,2,6]

[1]University of Bergen, Geophysical Institute, Bergen, Norway
[2]Bjerknes Centre for Climate Research, Bergen, Norway
[3]Institute of Marine Research, Bergen, Norway
[4]British Antarctic Survey, Cambridge, UK
[5]World Data Center for Marine Environmental Sciences, Bremen, Germany
[6]Uni Bjerknes Centre, Uni Research, Bergen, Norway

Received: 30 September 2011 – Accepted: 9 October 2011 – Published: 20 October 2011

Correspondence to: J. F. Tjiputra (jerry.tjiputra@bjerknes.uib.no)

Published by Copernicus Publications on behalf of the European Geosciences Union.

Abstract

A coupled biogeochemical-physical ocean model is used to study the long term variations of surface pCO_2 in the North Atlantic Ocean. The model agrees well with recent underway pCO_2 observations from the Surface Ocean CO_2 Atlas (SOCAT) database in various locations in the North Atlantic. The distinct seasonal cycles observed at different parts of the North Atlantic are well reproduced by the model. In most regions except the subpolar domain, the recent observed trends in pCO_2 and air–sea carbon fluxes are also simulated by the model. Over a long period between 1960–2008, the primary mode of surface pCO_2 variability is dominated by the increasing trend associated with the invasion of anthropogenic CO_2 into the ocean. We show that, to first order, the ocean surface circulation and air–sea heat flux patterns can explain the spatial variability of this dominant increasing trend. Regions with strong surface mass transport and negative air–sea heat flux have the tendency to maintain lower surface pCO_2. Regions of surface convergence and mean positive air–sea heat flux such as the subtropical gyre and the western subpolar gyre have faster increase in pCO_2 over a long term period. The North Atlantic Oscillation (NAO) plays a major role in controlling the variability occurring at interannual to decadal time scales. The NAO predominantly influences surface pCO_2 in the North Atlantic by changing the physical properties of the North Atlantic water masses, particularly by perturbing the temperature and dissolved inorganic carbon in the surface ocean. We show that present underway observations are valuable for both calibrating the model, as well as for improving our understanding of the regionally heterogeneous variability of surface pCO_2. In addition, they can be important for detecting any long term change in the regional carbon cycle due to ongoing climate change.

BGD

8, 10187–10227, 2011

1 Introduction

Future climate change will depend on the evolution of the atmospheric CO_2 concentration, which has been perturbed considerably by human activity during the past centuries. Studies have confirmed that less than half of the total anthropogenic CO_2 emitted over the anthropocene era due to burning of fossil fuels, land use change, and cement production remain in the atmosphere today (e.g., Canadell et al., 2007; Le Quéré et al., 2009). The rest is taken up by the terrestrial and ocean reservoirs mainly through plant photosynthesis and dissolution into seawater, respectively. The anthropogenic carbon uptake rate, however, is inhomogeneous and depends strongly on other external forcings acting on different spatial and temporal scales. In the ocean, the carbon uptake is influenced by processes ranging from short term biological activity to long term climate variability.

The North Atlantic ocean is an important region for oceanic carbon uptake. Takahashi et al. (2009) show that the most intense CO_2 sink area of the world oceans is located in the North Atlantic (for reference year 2000). Because of this many studies, both observational and modeling, in the past decade have been dedicated to better understand the variability of air–sea CO_2 fluxes in this region (e.g., Lefèvre et al., 2004; Lüger et al., 2006; Corbière et al., 2007; Thomas et al., 2008; Ullman et al., 2009; Watson et al., 2009; McKinley et al., 2011). In addition to altering the physical properties such as temperature and ocean circulation of the North Atlantic basin, climate change will also feedback onto the biogeochemical processes by influencing the surface carbon chemistry and biological processes, crucial for the oceanic carbon uptake. Therefore, understanding the role of present climate variability in controlling the North Atlantic carbon uptake remains a fundamental challenge and a necessary step in order to reduce the uncertainty associated with future climate projections.

On a time scales of less than one year, the air-sea CO_2 fluxes in the North Atlantic are controlled by the seasonal variability of biological processes, temperature, and mixed layer depth (e.g., Lefèvre et al., 2004; Olsen et al., 2008; Bennington et al.,

BGD
8, 10187–10227, 2011

2009). For interannual and decadal timescales, the long term change in the physical parameters associated with ocean circulation and climate variability dominates. The leading mode of climate variability in the North Atlantic is the North Atlantic Oscillation (NAO) (Hurrell and Deser, 2009). In this study, we assess the seasonal variability of the surface pCO_2 simulated by an ocean biogeochemical general circulation model (OBGCM) as compared to available observations. In addition, we apply a principal component statistical analysis to identify the primary and secondary mode of the surface pCO_2 variability over the North Atlantic basin over the 1960–2008 period. While the study by Thomas et al. (2008) has assessed the oceanic carbon uptake variability associated with the NAO, our study applies a different technique and covers a longer period in time.

Since the partial pressure of surface CO_2 (i.e., pCO_2) is one of the carbon parameters that is directly measurable and can be closely linked to the oceanic carbon uptake, we focus on the pCO_2 for the comparison between model results and observations. Furthermore, with the advancement of measurement techniques, in the last few years, autonomous pCO_2 measurement systems have been installed in many voluntary observing ships (VOS) to monitor the seawater pCO_2 (Pierrot et al., 2009). Resulting from this is substantial increase in the number of ship-based surface pCO_2 measurements with relatively high coverage both in space and time (Watson et al., 2009). In certain regions, the number of ship tracks increase to a point where month-to-month measurements can be compiled. This allows further insight into understanding the spatial and temporal variations of carbon dynamics in the North Atlantic region.

Another motivation for this study is to evaluate whether or not the governing processes behind the ocean carbon cycle model used in this study are sufficient to simulate the observed spatial and temporal pCO_2 variability in the North Atlantic. Basin-wide characteristics of key ocean carbon cycle variability will further be studied. This is an essential step because the model will be integrated into an Earth system model framework (e.g., Tjiputra et al., 2010a) and used to project future variability related to the climate change. Full assessment of the model, thus, will reduce the uncertainties

BGD
8, 10187–10227, 2011

and provide more confidence in future projections of the climate system and its associated carbon cycle feedback. It also serves as a prerequisite to test whether the model provides an appropriate first guess for use in advanced data assimilation schemes for more detailed global and regional predictions and optimisation of governing parameters of the carbon cycle.

The paper is organized as follows: in the next two sections we describe the observations and model used in this study. Section four discusses the results of the experiment analysis, and the study is summarized in section five.

2 Observation

In order to evaluate the model simulation, two independent data sets are employed. The first is from the CARINA (CARbon dioxide IN the Atlantic Ocean) data synthesis project which can be downloaded from http://cdiac.ornl.gov/oceans/CARINA/ (Velo et al., 2009; Key et al., 2010; Pierrot et al., 2010; Tanhua et al., 2010). It is comprised of quality-controlled observation from 188 cruises focusing on carbon-related parameters. For the model comparison, we extracted the surface measurements of temperature (SST), salinity (SSS), dissolved inorganic carbon (DIC), and alkalinity (ALK) over the North Atlantic domain between 1990 and 2006. The data is then averaged and binned into monthly fields with 1° by 1° horizontal resolution.

The second data set are observations of underway surface fCO_2 (i.e., fugacity of CO_2) extracted from the Surface Ocean CO_2 Atlas (SOCAT, Pfeil et al., 2011). SOCAT is the latest and most comprehensive surface ocean fCO_2 data base, containing 6.3 million fCO_2 values from 1851 voyages carried out during the time span between 1968 and 2007. SOCAT contains only measured fCO_2 data (i.e., not calculated from, for example, dissolved inorganic carbon and total alkalinity data). The data have been predominantly analyzed through infrared analysis of a sample of air in equilibration with a continuous stream of seawater (Pierrot et al., 2009), but some of the older data were measured using an automated gas chromatographic system (Weiss, 1981). We selected SOCAT data which has an overall accuracy of 4–5 µatm.

BGD
8, 10187–10227, 2011

In this study, we focus on the data sub-set from the North Atlantic basin. Figure 1 shows all the ship tracks that contain some measurements. Since the data is mainly used for comparison with the model in the seasonal time scale, we isolate regions with a good seasonal (i.e., at least 8 out of 12 months) coverage over continuous years. In addition, we also avoid regions close to the continental margins where the model does not perform adequately due to its fairly coarse resolution. Based on these criteria, we found three regions, each within a 4° by 4° horizontal domain (as shown by the white rectangle in Fig. 1), with reasonable seasonal coverage. To standardize the analysis, we use all data from these three locations spanning the 2002 to 2007 period for comparison with the model simulation.

The first region, centered at 60° N 32° W, is located in the subpolar gyre (NASPG) and was mainly covered by the routes of MV Skogafoss (processed by the United States, http://www.aoml.noaa.gov/ocd/gcc/skogafoss_introduction.php) and MV Nuka Arctica of the Danish Royal Arctic Lines (Olsen et al., 2008). The second region is located in the Northeast North Atlantic and was covered by the several VOS lines operated by Germany (Steinhoff, 2010), France, Spain (González Dávila et al., 2005; Padin et al., 2010), the UK (Schuster and Watson, 2007) and the United States, and is centered at 44° N 17° W (NE-ATL). The last location is close to the Caribbean and is covered by routes of reserch vessels from Germany, United States, Spain, and the UK, centered at 22° N 52° W (Caribbean). The three sub-domains represent different types of oceanic provinces from low- to high-latitudes.

In addition to underway observations, the pCO_2 data set from the Bermuda Atlantic Time series Station (BATS, 31°40″ N, 64°10″ W) (Bates, 2007) is also used as additional model validation. The addition of BATS is useful as it is one of the best studied ocean locations. For the purpose of this study, we only use data from the same period as the underway observations (i.e., 2002–2007).

BGD
8, 10187–10227, 2011

3 Model

In this study, we use a global coupled physical–biogeochemical ocean model (Assmann et al., 2010). The physical component is the dynamical isopycnic vertical coordinate MICOM ocean model (Bleck and Smith, 1990; Bleck et al., 1992), which includes some modifications as described in Bentsen et al. (2004). The horizontal resolution is approximately $2.4^\circ \times 2.4^\circ$ with grid spacing ranging from 60 km in the Arctic and Southern Ocean to 180 km in the subtropical regions. Vertically, the model consists of 34 isopycnic layers. In the additional topmost layer, the model adopts a single non-isopycnic surface mixed layer, and its depth is computed according to formulation by Gaspar (1988). This temporally and spatially varying mixed layer provides the linkage between the atmospheric forcing and the ocean interior.

The ocean carbon cycle model is the Hamburg Oceanic Carbon Cycle (HAMOCC5) model, which is based on the original work of Maier-Reimer (1993). The model has since then been improved extensively and has been used in many studies (Six and Maier-Reimer, 1996; Heinze et al., 1999; Aumont et al., 2003; Maier-Reimer et al., 2005). The current version of the model includes an NPZD-type ecosystem model, a 12-layer sediment module, full carbon chemistry, and multi-nutrient co-limitation of the primary production. The surface pCO_2 in the model is computed based on the prognostic temperature, salinity, pressure, dissolved inorganic carbon, and alkalinity. For the air–sea gas exchange, the model adopts the formulation of Wanninkhof (1992). A detailed description of the isopycnic version of HAMOCC is given by Assmann et al. (2010).

The model simulations performed in this study are forced by the daily atmospheric fields from the NCEP Reanalysis data set (Kalnay et al., 1996). For the air–sea CO_2 flux computation, the model prescribes observed atmospheric CO_2 concentration (instead of the observed emissions) from Mauna Loa observatory in Hawaii, which is a reasonable proxy for global mean concentration (Gammon et al., 1985). In general, the model reproduces well the amplitude and seasonal variabilities of the observed

BGD
8, 10187–10227, 2011

SST in all three North Atlantic locations as well as BATS (supplement Fig. 1). During winter the model tends to have a deeper mixed layer depth (MLD) than is observed, which may be attributed to the slightly cooler SST as compared to the observation. A more detailed evaluation of the model performance with respect to the global physical and carbon cycle parameters is also documented in Assmann et al. (2010).

4 Results

For the basin scale comparison with the CARINA data, the model-data fit is summarized in a Taylor diagram (Taylor et al., 2001) shown in Fig. 2. The Taylor diagram gives a statistical summary of how well the model simulated tracer distributions match the observed ones in term of correlation, standard deviations, and root-mean-square-difference (RMSD). Note that we only apply the surface data set (five meter and above) for this comparison because the main focus of this study is to study the surface pCO_2 variability. Figure 2 shows that the model simulated temporal and regional variabilities are generally close to the observation. The model simulated SST, SSS, DIC and ALK distributions have significant (within 95 % confidence interval) correlations of 0.77, 0.65, 0.73, and 0.69, respectively with the observations.

4.1 Regional seasonality of fCO_2

In this subsection we analyze the surface fCO_2 seasonal variability for the different sub-domains in the North Atlantic. The model simulated pCO_2 is converted into fCO_2 by using a conversion factor of 0.3 % (Weiss, 1974). Figure 3 compares the seasonal variability of surface fCO_2 taken from the underway measurements as well as from the BATS station together with the model simulations. For all regions, except for the Northeast Atlantic, the model broadly agrees with the observation in term of the amplitude of the seasonal cycle, with slightly shifted phase (e.g., in the NASPG region).

BGD
8, 10187–10227, 2011

To further identify the sources of the differences in seasonal variability between the model and data, we also separate the fCO_2 variability into temperature-driven (fCO_2-T) and non temperature-driven (fCO_2-nonT) variability following Takahashi et al. (2002). The fCO_2-T represents the temperature-controlled variability, as colder water has higher CO_2 solubility, thus lower fCO_2, whereas the opposite is true for warmer water. The fCO_2-nonT is composed of variability associated with alkalinity, SSS, and DIC variations throughout the year. Anomalies of both the fCO_2-T and fCO_2-nonT monthly variability from the observations and model are shown in Fig. 4 for each studied region.

For the NASPG region, the observations indicate a clear seasonal signal with winter maximum and summer minimum, consistent with earlier analyses (Olsen et al., 2008) for this region. The model also simulates pronounced seasonal variations with an amplitude close to the observations, but with its seasonal phase shifted by approximately two months. Based on the observations, Olsen et al. (2008) describe that the seasonal variability in this location is mostly dominated by upward mixing of DIC-rich water to the surface in the winter and by strong biological consumption throughout spring and summer. Consistently, Fig. 4 also shows similar observed patterns, with a weaker amplitude of the variability for fCO_2-T than fCO_2-nonT in the NASPG. The model shows good agreement with the observations in terms of fCO_2-T variability. The fCO_2-nonT phase-shift in the model is predominantly attributed to the simulated timing and dynamic of biological processes. In the early spring period, the increase in temperature and light availability lead to an accelerated simulated phytoplankton growth, which immediately consumes most of the nutrient upwelled during the previous winter. As a result, the nutrients become depleted and weak nutrient regeneration over the summer season is insufficient to maintain the steady biological consumption as observed (see Supplemental Fig. 2). During this period, the temperature effect simulated by the model prevails where an increase in temperature brings up the simulated pCO_2 back to its winter high values (see Fig. 3). On the contrary, the observational-based study by Olsen et al. (2008) suggests that the biological drawdown of DIC is maintained over

BGD
8, 10187–10227, 2011

the summer and dominates the increasing summer temperature. Consistent with the observations shown here, they found minimum fCO_2 values between 325–340 µatm during the summer. Simulating the correct ecosystem dynamics at high latitudes is a well known problem in global models as most models calibrate their ecosystem model towards time-series stations such as BATS, which are biased toward the subtropical regions (Tjiputra et al., 2007). A recent one-dimensional ecosystem model study by Signorini et al. (2011) shows that more sophisticated multi-functional groups of phytoplankton may be necessary to reproduce the biological carbon uptake during summer in the Icelandic waters close to where the NASPG domain is located.

The Northeast Atlantic station is located in between the North Atlantic subpolar and subtropical gyres. It is therefore expected that the variability here is dominated by both temperature variability as well as surface DIC dynamics. The observations suggest that the fCO_2-T and fCO_2-nonT variability are equally important and nearly cancel each other resulting in a relatively weak seasonal cycle (e.g., compared to that in the sub-polar region), as shown in Fig. 3. The study by Schuster and Watson (2007) over a somewhat larger ship-based observational region (30° W–5° W and 39° N–50° N) also shows similar weak seasonal fCO_2 variability in the early 2000s. The observations show two time intervals with maximum fCO_2: during late winter and late summer. Figure 4 shows that the late winter maximum is associated to the dynamics of surface DIC (nonT effect) whereas the late summer maximum is dominated by the temperature variations (i.e., maximum SST around the August and September months). The model is able to simulate the observed fCO_2-T seasonal cycle relatively well but the simulated fCO_2-nonT is considerably weaker. The model fCO_2 variability in this location looks very similar to that at the BATS station (see Fig. 4). As described above, this artefact is potentially due to the ecosystem dynamics biased toward the one at BATS. Another explanation for the model-data mismatch is because the due to the coarse resolution of the model, the location of the North Atlantic current (which is important for this domain) is not correctly simulated by the model.

BGD
8, 10187–10227, 2011

In the Caribbean sub-domain, both model and observations show the lowest seasonal variability of surface fCO_2 as compared to the other regions (Fig. 3). This is a general feature for low latitude regions (e.g., Watson et al., 2009). Figure 4 shows that variations in surface temperature are the main driver for the seasonal fluctuations, consistent with an earlier observational study over the same domain (Wanninkhof et al., 2007). Consequently, maximum surface fCO_2 occurs in the summer period when SST is high, and the minimum fCO_2 is observed during winter. The smaller role of fCO_2-nonT in this location can be attributed to the relatively weak seasonal variations in both the observed chlorophyll (i.e., biological activity) and mixed layer depth (Behrenfeld et al., 2005; de Boyer Montégut et al., 2004).

A study by Bates et al. (1996) reported that the surface waters at BATS are supersaturated with respect to CO_2 during the stratified summer months and undersaturated during the strong mixing in wintertime. Figure 3 shows that the model is able to simulate the observed mean seasonal variability in terms of both phase and amplitude. While there is a pronounced seasonality in the surface DIC (i.e., upwelling of DIC-rich subsurface water mass during the winter and biological production in the summer), both the model and observations agree in that the fCO_2-T variability dominates the seasonal variations (see Fig. 4). The seasonal SST variation at BATS is as large as that in the NASPG but the seasonal Net Primary Production (NPP) cycle remains much weaker (as shown in Supplemental Figs. 1 and 2). This dominant control of SST on the surface fCO_2 at BATS has also been shown by Gruber at al. (2002) for the period prior to the year 2000. Thus, similar to the Caribbean station, the fCO_2-nonT at BATS has only minor contributions.

4.2 Regional trends in fCO_2 and sea-air CO_2 flux

In this subsection, we compare the model simulated trend with estimates from observation. Annual trends of SST, SSS, fCO_2, and CO_2 flux for the 2002–2007 periods were computed from the observations and model results using linear least squares methodology. First, the seasonal cycle is removed from both the model and observation (i.e.,

BGD
8, 10187–10227, 2011

seasonally filtered) by substracting the monthly mean values from the data sets. We estimate the CO_2 flux from the observations following the formulation of Wanninkhof (1992), and the CO_2 solubility formulation of Weiss (1974). In situ SST and SSS are used for the solubility computation. When SSS is unavailable, a climatology from the World Ocean Atlas (WOA) data is used. NCEP monthly wind speed is used to compute the gas transfer rate. Finally, monthly atmospheric CO_2 concentration observed at Mauna Loa observatory is applied as a proxy of atmospheric pCO_2 boundary condition over each stations.

Table 1 shows that both the observations and the model consistently produce the same trend signals for SST and SSS, though the magnitude is weaker in the model. As decribed in Assmann et al. (2010), in order for the model to maintain a stable and realistic Atlantic Meridional Overturning Circulation (AMOC), a Newtonian relaxation is applied to the SST and SSS parameters in the model. For the simulation in this study, the SST and SSS ate relaxed at time scales of 180 and 60 days, respectively. This may explains the much weaker trend simulated by the model as compared to the observations, particularly for SSS. For most stations, except BATS, warming trends are estimated by both the model and the observations. There are only small changes in the surface salinity in all stations.

The seasonally filtered trends of surface fCO_2 and sea-air CO_2 fluxes in the four locations of North Atlantic are shown in Fig. 5. After the seasonal signals are removed from the time-series, the model's amplitude of the interannual variability agrees reasonably well with the observations, with higher variability being more pronounced in high latitudes. Both the model and the observations suggest that surface fCO_2 interannual variability ranges within $\pm 30\,\mu atm$ for nearly all regions. The amplitude of the interannual variability of the sea-air CO_2 fluxes varies from one region to the other, with the strongest variability shown at high latitude (i.e., NASPG), and the weakest at low latitude (i.e., Caribbean).

Over the 2002–2007 period, the model shows a positive trend of surface fCO_2 in all stations consistent with the observational estimates, except for the NASPG station

BGD
8, 10187–10227, 2011

where the observations indicate a negative trend. This is interesting as a previous study estimated that the surface fCO_2 around the NASPG domain has increased relatively faster (e.g., over 1990–2006 period) than in other regions in the North Atlantic (Corbière et al., 2007; Schuster et al., 2009). The observed negative trend in the NASPG domain can be attributed to the unusually low summer fCO_2 in 2007, which is not reproduced by the model. This anomalously low fCO_2 value is recorded despite the fact that both model and observation indicate a positive anomaly in SST (not shown) during the summer of 2007 relative to the previous summer periods, as also shown in Table 1 (i.e., a warming trend in SST). Therefore, the anomalously low summer fCO_2 in 2007 may be attributed to the other factors, such as the unusually high summer biological production as seen from observationally-derived estimates (Behrenfeld and Falkowski, 1997). And due to the model deficiency in maintaining high summer productivity in this location (supplement Fig. 2), it is unable to reproduce the anomalously low fCO_2 value. Interestingly, a modeling study by Oschlies (2001) suggests only a small increase in the nutrient concentration in this region under a positive NAO-phase (2007 is a dominant positive NAO phase year).

The respective observed atmospheric CO_2 trend for the same period is $2.031\,\mathrm{ppm\,yr^{-1}}$. Due to this opposing trend, it is not surprising that the observed sea-air carbon flux in the NASPG has a large negative trend (i.e., larger ocean carbon uptake) of $-0.284\,\mathrm{mol\,C\,m^{-2}\,yr^{-1}}$. The model on the other hand suggests a very small positive trend (i.e., less uptake) despite lower increase in surface ocean pCO_2 than in atmospheric. This is partially attributed by the negative trend in the spring surface wind speed in the region (not shown), which leads the model to simulate weaker atmospheric carbon uptake over time. Note that for the NASPG location, the model simulates the largest sea-air fCO_2 difference during the spring season as shown in Fig. 3.

At the Northeast Atlantic and Caribbean stations, the simulated positive surface fCO_2 trends compare favourably with the observations. Both the model and observations in the Northeast Atlantic suggest a stronger increase in oceanic fCO_2 than in the atmosphere, which translates into a weak positive trend in the sea-air CO_2

BGD
8, 10187–10227, 2011

fluxes (see Fig. 5). At the Caribbean station, the fCO_2 trends are weaker than the atmospheric value and therefore the CO_2 fluxes are weakly decreasing as well. The opposing signals in CO_2 fluxes between the two regions are also consistent with a recent observational-based estimate (covering a broader spectrum of VOS ship tracks between northwestern Europe and the Caribbean) that suggest a positive trend in carbon uptake followed by a negative one over the 2002–2007 period (Watson et al., 2009), resulting in small net change over the region.

The fCO_2 trends at BATS computed from the measurements and the model are both positive. However, the signal is much stronger in the observations, resulting in a negative trend in oceanic carbon sink. The model fCO_2 trend, on the other hand, is weaker than the corresponding atmospheric trend, and the model therefore simulates increasing carbon uptake in this location. Consistent with our model result, a study by Ullman et al. (2009) also suggests a relatively smaller increase in surface pCO_2 at the BATS station compared to the rest of the North Atlantic region, although their trend extends over the 1992–2006 period.

4.3 Basin scale trends and variability

Previous subsections show that, despite its deficiencies, the model is able to reasonably capture the seasonal variability and short-term trends observed in different regions in the North Atlantic basin. Here, we attempt to explain the regional variations in the surface pCO_2 simulated by the model and, to some extent, the observed ones. First, we analyze the dominant primary and secondary modes of long-term interannual variability of simulated surface pCO_2 over the 1960–2008 period. To do this, we first removed the mean pCO_2 value from each model grid point to yield the simulated pCO_2 anomaly. A principal component statistical analysis (von Storch and Zwiers, 2002) was then applied to these anomalies. Figure 6 shows the first empirical orthogonal function (EOF1) and the associated principal component (PC1) of the simulated annual surface pCO_2 anomaly over the 1960–2008 period. The first EOF explains 98 % of the overall model variance. The first principal component is plotted together with anomalies of

BGD
8, 10187–10227, 2011

model simulated annual pCO_2 and atmospheric CO_2 concentration observed at the Mauna Loa station. Multiplying the EOF1 value with the PC1 time-series yields the primary mode of surface pCO_2 variability simulated by the model. The temporal variability of PC1 indicates a dominant positive trend that correlates strongly with the observed atmospheric CO_2 anomaly ($r = 0.99$). This suggests that the primary temporal variability of surface pCO_2 in the model is mainly due to the anthropogenic carbon invasion into the seawater. Therefore, at regional scales and in the long run, the ocean pCO_2 follows the atmosphere.

For the above reason, the EOF1 map shown in Fig. 6 indicates regions where the anthropogenic CO_2 significantly affects the surface pCO_2 concentration. The main reason for the regional differences in the magnitude of surface pCO_2 increasing trend can be explained by the surface transport and air–sea heat flux patterns. The anthropogenic carbon taken up by the surface ocean is advected by the ocean circulation at the surface and transported into the deep by mixing and deep water formation processes (Tjiputra et al., 2010b). Figures 7 and 8 show the mean lateral ocean surface velocity and air–sea heat flux simulated by the model over the 1960–2008 period. In regions with strong mass transport, such as the Gulf Stream, the relatively warm water mass from the subtropic is advected northward and looses heat to the atmosphere. Here, the cooling of surface temperature increases the CO_2 gas solubility and translates into lower surface pCO_2 for the same dissolved inorganic carbon content. Thus, along the 30° N and 45° N, where the water is continuously transported northeastward into the Nordic Seas by the North Atlantic drift water, the surface pCO_2 increases relatively slower than the atmospheric CO_2 as illustrated in Fig. 6. In contrast, in the western subpolar gyre along 50° N latitude, the water mass here is transported southward from the Labrador Sea and warmed up by the atmosphere. Hence, the surface pCO_2 in this region increases relatively faster than the atmospheric CO_2.

Consistently, a recent study by Tjiputra et al. (2010b) using a fully coupled Earth system model shows that future anthropogenic carbon uptake in the North Atlantic regions is well confined to the North Atlantic drift current region. Convergence regions

BGD
8, 10187–10227, 2011

such as the subtropical Atlantic convergence zone is marked by a stronger increase in surface pCO_2 as less anthropogenic CO_2 is laterally advected away from this area (Fig. 7) and there is a net heat gain in this region (Fig. 8). Both the Greenland and the Norwegian Seas represent some of the oldest surface water masses before they are transported to the deep water (i.e., have resided for a long period close to the sea surface), which also explains the relatively high anthropogenic CO_2 concentration simulated in the model. On the western coast of North Africa, the anomalously lower contribution of anthropogenic CO_2 can be explained by the fact that this is an upwelling region, where the water mass is less exposed to the anthropogenic CO_2.

The magnitude of PC1 shown in Fig. 6b is standardized to be comparable to the observed atmospheric CO_2 anomaly. Therefore, the map of EOF1 can be used to approximate the strength of increasing surface pCO_2 trend relative to the atmospheric CO_2 trend. Values greater (less) than one suggest increasing surface pCO_2 faster (slower) than the atmospheric CO_2 partial pressure. Note that this trend and these variations occur over a much longer period than recent observational studies. Thus, in order to understand and compare the trend in this study with relatively shorter trend resulted from the observational study, a further analysis on the short term interannual climate variability is required.

To understand the shorter term mode variability, we compute the second mode variability simulated by the model. Figure 9 shows the EOF2, which gives the dominant variability of surface pCO_2 after the positive trend resulting from the anthropogenic CO_2 uptake (see Fig. 6b) is removed. Thus it explains the main variations due to physical climate variability over the 1960–2008 period. Figure 9b shows that the temporal variations of PC2 is reasonably well correlated with the North Atlantic Oscillation (NAO)-index (Hurrell and Deser, 2009) ($r = 0.557$). The NAO is a leading climate variability pattern over the North Atlantic, which affects, e.g., the heat content and circulation of the ocean. The correlation is stronger during strong NAO index events (i.e., when the NAO-index is greater than one standard deviation, $r = 0.747$). This second mode correlation with NAO variability is consistent with a previous study (Thomas et al., 2008),

BGD
8, 10187–10227, 2011

which shows that changes in wind-driven ocean circulation associated with the NAO variability influence the North Atlantic CO_2 system by altering the surface water properties.

The spatial pattern of EOF2 shown in Fig. 9 indicates that the second mode variability (approximately NAO-like) predominantly represents the interannual variability of surface pCO_2 in the North Atlantic sub-polar region, with opposite variability between the western and eastern parts. In the western sub-polar gyre, the model simulates positive anomalies of pCO_2 under positive NAO condition, whereas the negative anomalies is simulated in the eastern part of the sub-polar gyre.

In the model, the pCO_2 is determined as a function of surface temperature (SST), salinity (SSS), alkalinity, and dissolved inorganic carbon (DIC) concentrations. To quantify the influence of the NAO-variability on each of these parameters, we analyzed an earlier model simulation, which used the same atmospheric physical forcing, but maintained a preindustrial atmospheric CO_2 concentration (Assmann et al., 2010). This simulation, in principle, would have the positive pCO_2 trend associated with the anthropogenic effects, as shown in Fig. 6, removed from the system. Therefore, it can be better used to analyze the variability of the CO_2 system associated with the present climate variability. Next, we compute mean annual anomalies of the simulated SST, SSS, alkalinity, and DIC under the dominant positive and negative NAO phases between 1960–2007. The dominant NAO-phase is defined here as years when the absolute NAO-index is larger than one standard deviation. The computed annual anomalies are then used to construct a composite of the surface pCO_2 anomalies attributed to changes in these parameters under both positive and negative NAO condition, as shown in Fig. 10. For example, to compute the SST-attributed pCO_2 anomaly (i.e., pCO_2-SST), we compute the pCO_2 applying the SST anomalies together with the mean values of SSS, alkalinity, and DIC simulated by the model. For the pCO_2 computation here, we use the Matlab code provided by Zeebe and Wolf-Gladrow (2001).

In the North Atlantic, the surface temperature has been recognized to vary with respect to the dominant NAO variability (Hurrell and Deser, 2009). The model simulates

BGD
8, 10187–10227, 2011

well the expected tri-polar SST anomalies as a direct result of the anomalous air–sea heat fluxes associated with the different NAO-modes (Marshall et al., 2001), which also have been shown to persist for about a year (Watanabe and Kimoto, 2000). Under a positive NAO-mode, the tri-polar structure consists of the following: a cold anomaly in the subpolar North Atlantic due to the enhanced northerly cold Arctic air masses, which results in net sea-to-air heat loss, and in the mid latitudes, stronger westerly flows moves relatively warm air mass and creating a warm anomaly in the region. A strong correlation between the SST and NAO-index in the North Sea is also shown, due to the NAO-dependent inflow of warmer and more saline Atlantic water mass into the region (Pingree, 2005) which is also reflected in the pCO_2-SSS component in Fig. 10. Finally, stronger clockwise flow over the subtropical Atlantic high leads to a negative SST anomaly to close the tri-polar structure. During the negative NAO-mode, approximately the opposite conditions prevail. Figure 10 shows that this regional change in SST translates into similar regional variability in the surface pCO_2 anomalies, with colder SST yielding negative pCO_2 anomalies whereas warmer SSTs yield the opposite. The strongest NAO-associated temperature effect on the surface pCO_2 occurs in the western part of the North Atlantic subpolar gyre. This region is recently shown in Corbière et al. (2007) and Metzl et al. (2010) to have a positive trend in surface pCO_2 predominantly attributed by the observed surface warming. For a similar period as their studies, i.e., 1993–2008, our model also simulates a surface pCO_2 trend between 2.0 and 2.5 µatm yr^{-1} in the same region. Figure 9 shows that the surface pCO_2 in this region (between Iceland and Northeastern Canada) is reasonably well (negatively) correlated with the NAO-index. Since the NAO-phase is moving from dominant positive (1993) into more neutral phases, we would expect to have increasing pCO_2 as mentioned above. Other regions strongly affected by the temperature variability, such as the eastern part of the subpolar gyre and along the North Atlantic drift region, are damped by the opposing pCO_2-DIC variability, as described below.

Due to the relaxation applied to the SSS in the model, there are very weak year-to-year salinity variations. Therefore, the salinity in the model has relatively smaller effect

BGD
8, 10187–10227, 2011

than the other parameters in influencing the surface pCO_2 over most of the North Atlantic basin. A weak positive SSS anomaly during a strong positive NAO phase is simulated in the western part of the transition region between the subtropical and subpolar gyre (slightly south of 45° N), which is associated to the northward shift of the subtropical gyre transporting more saline water from the tropics. The opposite is seen during a negative NAO phase.

The variability of surface pCO_2 due to variations of alkalinity in the surface is generally small (Tjiputra and Wiguth, 2008). Figure 10 shows that under both dominant NAO-phases the pCO_2-ALK variability is most pronounced along the western coast of North Africa. Close to the North African coast, anomalously high trade winds during positive NAO phase (Visbeck et al., 2003) lead to enhanced nutrient upwelling and surface biological production. This is consistent with a study by Oschlies (2001), which shows that surface nutrient input in this region is enhanced by both vertical mixing and horizontal advection during dominant positive NAO phase. This NPP increase explains the lower pCO_2-alkalinity as biological production increase surface alkalinity, and thus reduce the pCO_2.

The DIC driven surface pCO_2 variability is very pronounced along the North Atlantic inter-gyre boundary region located along 45° N (i.e., between the North Atlantic subtropical and subpolar gyres). Stronger wind-forced surface water transport during a positive NAO phase leads to increase in supply of relatively low-DIC subtropical water, which induces a negative annual anomaly of pCO_2-DIC. The reverse is true for dominant negative NAO phase years. In the northeastern part of the North Atlantic subpolar gyre (i.e., approximately between 55° N–60° N and 25° W–30° W), strong cooling under a positive NAO phase deepens the winter MLD and upwells DIC-rich deep water, creating a positive pCO_2-DIC anomaly. On contrast, Thomas et al. (2008) show a negative ΔpCO_2 (reduced surface pCO_2) in this region during the early 1990s positive NAO period due to an increase in low-DIC water mass from the subtropical region. This disagreement may be attributed to the difference in the location of the North Atlantic drift simulated by the different models. In the southern part of the subpolar

BGD
8, 10187–10227, 2011

gyre (i.e., centered approximately around 50° N and 38° W), the pCO_2-DIC shows distinct variations between the two phases of NAO. Under dominant positive NAO years, stronger southward current from the Labrador Sea transports colder (as also shown in pCO_2-SST), DIC-rich water and leads to a positive pCO_2-DIC anomaly. Under a dominant negative NAO-phase, the model shows a clear opposite regional pattern. There is also a pronounced co-variation between the NAO and the pCO_2-DIC in the center of the subtropical gyre. Visbeck et al. (2003) show that the winter wind stress in this location is co-varying with the NAO, which is attributed to the slightly enhanced trade winds during positive NAO conditions. In the model, this relation translates into stronger surface DIC transport away from the region, creating a negative pCO_2-DIC anomaly. Consequently, the model also simulates a positive air–sea CO_2 flux anomaly (i.e., more carbon uptake) in this location during a dominant positive NAO phase (not shown). During a negative NAO phase, the opposite process occurs. Figure 9 shows that the DIC control of surface pCO_2 in the inter-gyre boundary is damped by the SST effect. Similarly, in the southern part of the subpolar gyre the pCO_2-SST overcomes the pCO_2-DIC variability. The strongest effects of pCO_2-DIC variability due to changes in the NAO-phase are taking effect in the eastern subpolar gyre and in the central subtropical gyre.

4.4 Monitoring future feedback

In the North Atlantic, Fig. 1 shows that there are three locations, where the frequency of the temporal coverage of underway fCO_2 measurements has considerably increased, particularly in the past decade. This is mostly due to the operation of autonomous pCO_2 instruments on well-established shipping lines between the Europe and the North America (Pfeil et al., 2011) and the fact that underway pCO_2 observation are relatively cost efficient compare to the traditional bottle data. It is not up to the CO_2 research community to decide the routes of commercial vessels and while these locations are not optimal (i.e., as suggested by our model), if the measurements are continued steadily, they may have the potential to monitor any emerging climate feedback on

BGD
8, 10187–10227, 2011

the carbon uptake in the future. In both Figs. 6a and 9a, these three locations shows that surface ocean pCO_2 generally increases at a rate following the atmospheric CO_2 increase (i.e., value close to one in Fig. 6a) but with short term deviations that depends on the NAO variability. Therefore, future measurements are useful to better understand any short term change in the surface pCO_2 trend recently observed in parts of the North Atlantic. For example, a recent study by Metzl et al. (2010) shows that observations of surface pCO_2 between the Iceland and Canada over the 1993–2008 indicate an positive trend faster than the atmosphere. This is consistent with Fig. 9, which shows that the region has negative correlation with the NAO index, and over the 1993–2008 the NAO index trend is negative.

To evaluate the potential of the monitoring system we have in place, the model is applied to compute the pCO_2 trend at the three locations as well as the BATS station during very strong shifts of NAO regimes. We focus on two periods: one with a strong shift from negative to positive (1969–1973) and one from positive to negative (1993–1997) NAO-indeces (see Fig. 9b). Table 2 summarizes the trends in surface pCO_2 as well as the sea-air CO_2 fluxes simulated by the model. During the 1969–1973 period of strong positive trend of NAO (strong shift from negative to positive), the NASPG, Northeast Atlantic, and Caribbean stations have weaker pCO_2 trends than the atmosphere. The trend in BATS more closely follows the atmospheric trend. Analogously, the model also simulates a negative CO_2 flux trend (more carbon uptake) in the NASPG and the Caribbean, whereas less carbon uptake (or more outgassing) is simulated at BATS. Interestingly, the model simulates a weak increase in outgassing (less uptake) in the Northeast Atlantic location. Since the model does not perform well compared to the observation in this location (see Figs. 3 and 4), it is more difficult to interpret the results. During the positive to negative shifts in the NAO index (1993–1997), the model shows the opposite signals, but with much stronger trends in surface pCO_2 at the three underway stations relative to the atmospheric CO_2 trend. Consequently, the sea-air CO_2 fluxes show positive trends (less uptake) for these locations. For the BATS station, our model shows the opposite signals for this period. This is consistent with earlier study

BGD
8, 10187–10227, 2011

by Gruber at al. (2002) who also show a dominant negative trend in CO_2 fluxes (more carbon uptake) for the 1993–1997 period.

5 Summary

In this study, we use a coupled ocean biogeochemical general circulation model to assess the long term variability of surface fCO_2 in the North Atlantic. We apply two independent data sets to validate the model simulation (CARINA and SOCAT). For most of the locations we select, the model is able to produce the correct amplitude of the observed seasonal cycle. In the North Atlantic subpolar gyre, the seasonal cycle phase in the model is slightly shifted compared to the observations, which can be attributed to the model deficiency in the surface biological processes. Additionally, the model broadly agrees with the observation in the interannual trend of surface fCO_2 and air–sea CO_2 fluxes.

Using a principal component analysis, we show that the primary variability of the surface pCO_2 simulated by the model over the 1960–2008 period is associated to the increasing trend of atmospheric CO_2. The spatial variability of this trend is predominantly influenced by the surface ocean circulation and air–sea heat flux patterns. Regions with steady mass transport heat loss to the atmosphere, such as the North Atlantic drift current, generally have weaker pCO_2 trends than the atmospheric CO_2. On contrast, convergence regions (e.g., subtropical gyres) or regions with large heat gain (e.g., western subpolar gyre) have a relatively larger trend than that observed from the atmospheric CO_2 concentration.

The analysis also reveals that over shorter interannual to decadal time scales, the variability of surface pCO_2 is considerably influenced by the NAO, the leading climate variability pattern over the North Atlantic. We also evaluate the physical and chemical mechanisms behind the NAO induced regional pCO_2 variations. The NAO associated temperature variability influences the surface pCO_2 variability, particularly in the western part of the subpolar gyre. In the intergyre boundary, the pCO_2 variations due to

BGD
8, 10187–10227, 2011

change in SST and DIC are almost equal in magnitude but in opposite directions, so they cancel each other. In the subtropical gyre, the change in wind stress in different NAO-regimes affects the transport of surface DIC, and hence alters the surface pCO_2. In general we find very little contributions from SSS and alkalinity to the overall pCO_2 variability.

Finally we show that, while not optimal, if the currently established shipping routes in the North Atlantic continue to record the surface pCO_2, they will have the potential to monitor any long term pCO_2 variability as well as solidify our understanding of climate-carbon cycle interactions in the North Atlantic basin.

Supplementary material related to this article is available online at: http://www.biogeosciences-discuss.net/8/10187/2011/bgd-8-10187-2011-supplement.pdf.

Acknowledgements. We thank Richard Bellerby for the review of the manuscript. This study at the University of Bergen and Bjerknes Centre for Climate Research is supported by the Research Council of Norway funded projects CarboSeason (185105/S30) and A-CARB (188167) and by the European Commission through funds from the EU FP7 Coordination Action Carbon Observing System COCOS (212196). We also acknowledge the Norwegian Metacenter for Computational Science and Storage Infrastructure (NOTUR and Norstore, "Biogeochemical Earth system modeling" project nn2980k and ns2980k) for providing the computing and storage resources.

References

Assmann, K. M., Bentsen, M., Segschneider, J., and Heinze, C.: An isopycnic ocean carbon cycle model, Geosci. Model Dev., 3, 143–167, doi:10.5194/gmd-3-143-2010, 2010. 10193, 10194, 10198, 10203

Aumont, O., Maier-Reimer, E., Blain, S., and Monfray, P.: An ecosystem model of the

BGD
8, 10187–10227, 2011

global ocean including Fe, Si, P colimitations, Global Biogeochem. Cy., 17, 1060, doi:10.1029/2001GB001745, 2003. 10193
Bates, N. R.: Interannual variability of the oceanic CO_2 sink in the subtropical gyre of the North Atlantic Ocean over the last 2 decades, J. Geophys. Res., 112, C09013, doi:10.1029/2006JC003759, 2007. 10192
Bates, N. R., Michaels, A. F., and Knap, A. H.: Seasonal and interannual variability of the oceanic carbon dioxide system at the US JGOFS Bermuda Atlantic Time-series Site, Deep-Sea Res. Pt. II, 43, 347–383, 1996. 10197
Behrenfeld, M. J. and Falkowski, P. G.: Photosynthetic rates derived from satellite-based chlorophyll concentration, Limnol. Oceanogr., 42, 1–20, 1997. 10199
Behrenfeld, M. J., Boss, E., Siegel, D. A., and Shea, D. M.: Carbon-based ocean productivity and phytoplankton physiology from space, Global Biogeochem. Cy., 19, GB1006, doi:10.1029/2004GB002299, 2005. 10197
Bennington, V., McKinley, G. A., Dutkiewicz, S., and Ullman, D.: What does chlorophyll variability tell us about export and air–sea CO_2 flux variability in the North Atlantic?, Global Biogeochem. Cy., 23, GB3002, doi:10.1029/2008GB003241, 2009. 10189
Bentsen, M., Drange, H., Furevik, T., and Zhou, T.: Simulated variability of the Atlantic meridional overturning circulation, Clim. Dynam., 22, 701–720, 2004. 10193
Bleck, R. and Smith, L. T.: A wind-driven isopycnic coordinate model of the North and Equatorial Atlantic Ocean. 1. Model development and supporting experiments, J. Geophys. Res., 95, 3273–3285, 1990. 10193
Bleck, R., Rooth, C., Hu, D., and Smith, L. T.: Salinity-driven thermocline transients in a wind- and thermohaline-forced isopycnic coordinate model of the North Atlantic, J. Pys. Oceanogr., 22, 1486–1505, 1992. 10193
de Boyer Montégut, C., Madec, G., Fischer, A. S., Lazar, A., and Iudicone, D.: Mixed layer depth over the global ocean: an examination of profile data and a profile-based climatology, J. Geophys. Res., 109, C12003, doi:10.1029/2004JC002378, 2004. 10197
Canadell, J. G., Le Quéré, C., Raupach, M. R., Field, C. B., Buitenhuis, E. T., Ciais, P., Conway, T. J., Gillett, N. P., Houghton, R. A., and Marland, G.: Contributions to accelerating atmospheric CO_2 growth from economic activity, carbon intensity, and efficiency of natural sinks, P. Natl. Acad. Sci. USA, 104, 18866–18870, 2007. 10189
Corbière, A., Metzl, N., Reverdin, G., Brunet, C., and Takahashi, T.: Interannual and decadal variability of the oceanic carbon sink in the North Atlantic subpolar gyre, Tellus B, 59, 168–

BGD
8, 10187–10227, 2011

179, doi:10.1111/j.1600-0889.2006.00232.x, 2007. 10189, 10199, 10204
Gammon, R., Sundquist, E., and Frazer, P.: History of carbon dioxide in the atmosphere, in atmospheric carbon dioxide and the global carbon cycle, Rep. DOE/ER-0239, US Dep. of Energy, Washington DC, 1985. 10193
Gaspar, P.: Modeling the seasonal cycle of the upper ocean, J. Phys. Oceanogr., 18, 161–180, 1988. 10193
González Dávila, M., Santana-Casiano, J. M., Merlivat, L., Barbero-Muños, L., and Dafner, E. V.: Fluxes of CO_2 between the atmosphere and the ocean during the POMME project in the Northeast Atlantic Ocean during 2001, J. Geophys. Res., 110, C07S11, doi:10.1029/2004JC002763, 2005. 10192
Gruber, N., Keeling, C. D., and Bates, N. R.: Interannual variability in the North Atlantic ocean carbon sink, Science, 298, 2374–2378, 2002. 10197, 10208
Heinze, C., Maier-Reimer, E., Winguth, A. M. E., and Archer, D.: A global oceanic sediment model for long-term climate studies, Global Biogeochem. Cy., 13, 221–250, 1999. 10193
Hurrell, J. W. and Deser, C.: North Atlantic climate variability: the role of the North Atlantic Oscillation, J. Mar. Syst., 78, 28–41, doi:10.1016/j.jmarsys.2008.11.026, 2009. 10190, 10202, 10203
Kalnay, E., Kanamitsu, M., Kistler, R., Collins, W., Deaven, D., Gandin, L., Iredell, M., Saha, S., White, G., Woollen, J., Zhu, Y., Chelliah, M., Ebisuzaki, W., Higgins, W., Janowiak, J., Mo, K. C., Ropelewski, C., Wang, J., Leetmaa, A., Reynolds, R., Jenne, R., and Joseph, D.: The NCEP/NCAR 40-yr reanalysis project, B. Am.. Meteorol. Soc., 77, 437–471, 1996. 10193
Key, R. M., Tanhua, T., Olsen, A., Hoppema, M., Jutterström, S., Schirnick, C., van Heuven, S., Kozyr, A., Lin, X., Velo, A., Wallace, D. W. R., and Mintrop, L.: The CARINA data synthesis project: introduction and overview, Earth Syst. Sci. Data, 2, 105–121, doi:10.5194/essd-2-105-2010, 2010. 10191
Lee, K., Tong, L. T., Millero, F. J., Sabine, C. L., Dickson, A. G., Goyet, C., Park, G.-H., Wanninkhof, R., Feely, R. A., and Key, R. M.: Global relationships of total alkalinity with salinity and temperature in surface waters of the world's oceans, Geophys. Res. Lett., 33, L19605, doi:10.1029/2006GL027207, 2006.
Lefèvre, N., Watson, A. J., Olsen, A., Rios, A. F., Pérez, F. F., and Johannessen, T.: A decrease in the sink for atmospheric CO_2 in the North Atlantic, Geophys. Res. Lett., 31, L07306, doi:10.1029/2003GL018957, 2004. 10189

BGD
8, 10187–10227, 2011

Le Quéré, C., Raupach, M. R., Canadell, J. G., Marland, G., Bopp, L., Ciais, P., Conway, T. J., Doney, S. C., Feely, R., Foster, P., Friedlingstein, P., Gurney, K., Houghton, R. A., House, J. I., Huntingford, C., Levy, P. E., Lomas, M. R., Majkut, J., Metzl, N., Ometto, J. P., Peters, G. P., Prentice, I. C., Randerson, J. T., Running, S. W., Sarmiento, J. L., Schuster, U., Sitch, S., Viovy, T. T. N., van der Werf, G. R., and Woodward, F. I.: Trends in the sources and sinks of carbon dioxide, Nat. Geosci., 2, 831–836, doi:10.1038/ngeo689, 2009. 10189

Lüger, H., Wanninkhof, W., Wallace, D. W. R., and Körtzinger, A.: CO_2 fluxes in the subtropical and subarctic North Atlantic based on measurements from a volunteer observing ship, J. Geophys. Res., 111, C06024, doi:10.1029/2005JC003101, 2006. 10189

Maier-Reimer, E.: Geochemical cycles in an ocean general circulation model, preindustrial tracer distributions, Global Biogeochem. Cy., 7, 645–677, 1993. 10193

Maier-Reimer, E., Kriest, I., Segschneider, J., and Wetzel, P.: The HAMburg Ocean Carbon Cycle Model HAMOCC5.1 – Technical Description Release 1.1, Berichte zur Erdsystemforschung 14, ISSN 1614–1199, Max Planck Institute for Meteorology, Hamburg, Germany, 50 pp., 2005. 10193

Marshall, J., Kushnir, Y., Batisti, D., Chang, P., Czaja, A., Dickson, R., Hurrell, J., McCartney, M., Saravanan, R., and Visbeck, M.: North Atlantic climate variability; phenomena, impacts and mechanisms, Int. J. Climatol., 21, 1863–1898, 2001. 10204

McKinley, G. A., Fay, A. R., Takahashi, T., and Metzl, N.: Convergence of atmospheric and North Atlantic carbon dioxide trends on multidecadal timescales, Nat. Geosci., 4, 606–610, doi:10.1038/ngeo1193, 2011. 10189

Metzl, N., Corbière, A., Reverdin, G., Lenton, A., Takahashi, T., Olsen, A., Johannessen, T., Pierrot, D., Wanninkhof, R., Ólafsdóttir, S. R., Olafsson, J., and Ramonet, M.: Recent acceleration of the sea surface fCO_2 growth rate in the North Atlantic subpolar gyre (1993–2008) revealed by winter observations, Global Biogeochem. Cy., 24, GB4004, doi:10.1029/2009GB003658, 2010. 10204, 10207

Olsen, A., Brown, K. R., Chierici, M., Johannessen, T., and Neill, C.: Sea-surface CO_2 fugacity in the subpolar North Atlantic, Biogeosciences, 5, 535–547, doi:10.5194/bg-5-535-2008, 2008. 10189, 10192, 10195

Oschlies, A.: NAO-induced long-term changes in nutrient supply to the surface waters of the North Atlantic, Geophys. Res. Lett., 28, 1751–1754, 2001. 10199, 10205

Padin, X. A., Vázquez-Rodríguez, M., Castaño, M., Velo, A., Alonso-Pérez, F., Gago, J., Gilcoto, M., Álvarez, M., Pardo, P. C., de la Paz, M., Ríos, A. F., and Pérez, F. F.: Air-Sea CO_2 fluxes in

BGD
8, 10187–10227, 2011

the Atlantic as measured during boreal spring and autumn, Biogeosciences, 7, 1587–1606, doi:10.5194/bg-7-1587-2010, 2010. 10192
Pfeil, B., Olsen, A., and Bakker, D. C. E.: A uniform, quality controlled Surface Ocean CO_2 Atlas (SOCAT), Earth Syst. Sci. Data, in preparation. 10191, 10206
Pierrot, D., Neill, C., Sullivan, K., Castle, R., Wanninkhof, R., Lüger, H., Johannessen, T., Olsen, A., Feely, R. A., and Cosca, C. E.: Recommendations for autonomous underway pCO_2 measuring systems and data-reduction routines, Deep-Sea Res. Pt. II, 56, 512–522, doi:10.1016/j.dsr2.2008.12.005, 2009. 10190, 10191
Pierrot, D., Brown, P., Van Heuven, S., Tanhua, T., Schuster, U., Wanninkhof, R., and Key, R. M.: CARINA TCO_2 data in the Atlantic Ocean, Earth Syst. Sci. Data, 2, 177–187, doi:10.5194/essd-2-177-2010, 2010. 10191
Pingree, R.: North Atlantic and North Sea climate change: curl up, shut down, NAO and ocean colour, J. Mar. Biol. Ass. UK, 85, 1301–1315, 2005. 10204
Schuster, U. and Watson, A. J.: A variable and decreasing sink for atmospheric CO_2 in the North Atlantic, J. Geophys. Res., 112, C11006, doi:10.1029/2006JC003941, 2007. 10192, 10196
Schuster, U., Watson, A. J., Bates, N. R., Corbiere, A., Gonzales-Davila, M., Metzl, N., Pierrot, D., and Santana-Casiano, M.: Trends in North Atlantic sea-surface fCO_2 from 1990 to 2006, Deep-Sea Res. Pt. II, 56, 620–629, doi:10.1016/j.dsr2.2008.12.011, 2009. 10199
Signorini, S. R., Häkkinen, S., Gudmundsson, K., Olsen, A., Omar, A. M., Olafsson, J., Reverdin, G., Henson, S. A., and McClain, C. R.: The role of phytoplankton dynamics in the seasonal variability of carbon in the subpolar North Atlantic - a modeling study, Geosci. Model Dev. Discuss., 4, 289–342, doi:10.5194/gmdd-4-289-2011, 2011. 10196
Six, K. D. and Maier-Reimer, E.: Effects of plankton dynamics on seasonal carbon fluxes in an ocean general circulation model, Global Biogeochem. Cy., 10, 559–583, 1996. 10193
Steinhoff, T.: Carbon and nutrient fluxes in the North Atlantic, Ph.D. thesis, Christian-Albrechts-Universität zu Kiel, Kiel, Germany, 162 pp., 2010. 10192
von Storch, H. and Zwiers, F. W.: Statistical Analysis in Climate Research, Pergamon, Oxford, UK, 442 pp., 2002. 10200
Takahashi, T., Sutherland, S. C., Sweeney, C., Poisson, A., Metzl, N., Tilbrook, B., Bates, N., Wanninkhof, R., Feely, R. A., Sabine, C., Olafsson, J., and Nojiri, Y.: Global sea-air CO_2 flux based on climatological surface ocean pCO_2, and seasonal biological and temperature effects, Deep-Sea Res. Pt. II, 49, 1601–1622, 2002. 10195

BGD
8, 10187–10227, 2011

Takahashi, T., Sutherland, S., Wanninkhof, W., Sweeney, C., Feely, R. A., Chipman, D. W., Hales, B., Friederich, G., Chavez, F., Sabine, C., Watson, A., Bakker, D. C. E., Schuster, U., Metzl, N., Yoshikawa-Inoue, H., Ishii, M., Midorikawa, T., Nojiri, Y., Körtzinger, A., Steinhoff, T., Hoppema, M., Olafsson, J., Arnarson, T. S., Tilbrook, B., Johannessen, T., Olsen, A., Bellerby, R., Wong, C. S., Delille, B., Bates, N. R., and de Baar, H. J. W.: Climatological mean and decadal change in surface ocean pCO_2, and net sea-air CO_2 flux over the global oceans, Deep-Sea Res. Pt. II, 56, 554–577, doi:10.1016/j.dsr2.2008.12.009, 2009. 10189

Tanhua, T., Steinfeldt, R., Key, R. M., Brown, P., Gruber, N., Wanninkhof, R., Perez, F., Körtzinger, A., Velo, A., Schuster, U., van Heuven, S., Bullister, J. L., Stendardo, I., Hoppema, M., Olsen, A., Kozyr, A., Pierrot, D., Schirnick, C., and Wallace, D. W. R.: Atlantic Ocean CARINA data: overview and salinity adjustments, Earth Syst. Sci. Data, 2, 17–34, doi:10.5194/essd-2-17-2010, 2010. 10191

Taylor, K. E.: Summarizing multiple aspects of model performance in a single diagram, J. Geophys. Res., 106, 7183–7192, 2001. 10194

Thomas, H., Friederike Prowe, A. E., Lima, I. D., Doney, S. C., Wanninkhof, R., Greatbatch, R. J., Schuster, U., and Corbiére, Changes in the North Atlantic Oscillation influence CO_2 uptake in the North Atlantic over the past 2 decades, Global Biogeochem. Cy., 22, GB4027, doi:10.1029/2007GB003167, 2008. 10189, 10190, 10202, 10205

Tjiputra, J. F. and Winguth, A. M. E.: Sensitivity of sea-to-air CO_2 flux to ecosystem parameters from an adjoint model, Biogeosciences, 5, 615–630, doi:10.5194/bg-5-615-2008, 2008. 10205

Tjiputra, J. F., Polzin, D., and Winguth, A. M. E.: Assimilation of seasonal chlorophyll and nutrient data into an adjoint three-dimensional ocean carbon cycle model: Sensitivity analysis and ecosystem parameter optimization, Global Biogeochem. Cy., 21, GB1001, doi:10.1029/2006GB002745, 2007. 10196

Tjiputra, J. F., Assmann, K., Bentsen, M., Bethke, I., Otterå, O. H., Sturm, C., and Heinze, C.: Bergen Earth system model (BCM-C): model description and regional climate-carbon cycle feedbacks assessment, Geosci. Model Dev., 3, 123–141, doi:10.5194/gmd-3-123-2010, 2010a. 10190

Tjiputra, J. F., Assmann, K., and Heinze, C.: Anthropogenic carbon dynamics in the changing ocean, Ocean Sci., 6, 605–614, doi:10.5194/os-6-605-2010, 2010b. 10201

Ullman, D. J., McKinley, G. A., Bennington, V., and Dutkiewicz, S.: Trends in the North Atlantic carbon sink: 1992–2006, Global Biogeochem. Cy., 23, GB4011,

BGD
8, 10187–10227, 2011

doi:10.1029/2008GB003383, 2009. 10189, 10200
Velo, A., Perez, F. F., Brown, P., Tanhua, T., Schuster, U., and Key, R. M.: CARINA alkalinity data in the Atlantic Ocean, Earth Syst. Sci. Data, 1, 45–61, doi:10.5194/essd-1-45-2009, 2009. 10191
Visbeck, M., Chassignet, E. P., Curry, R. G., Delworth, T. L., Dickson, R. R., and Krahmann, G.: The ocean's response to North Atlantic Oscillation variability, in: The North Atlantic Oscillation, Climate Significance and Environmental Impact, edited by: Hurrell, J. W., Kushnir, Y., Ottersen, G., Visbeck, M., AGU Geophysical Monograph, 134, American Geophysical Union, Washington, DC, 113–146, 2003. 10205, 10206
Wanninkhof, R.: Relationship between wind speed and gas exchange over the ocean, J. Geophys. Res., 97, 7373–7382, 1992. 10193, 10198
Wanninkhof, R., Olsen, A., and Triñanes, J.: Air-sea CO_2 fluxes in the Caribbean Sea from 2002–2004, J. Mar. Sys., 66, 272–284, doi:10.1016/j.jmarsys.2005.11.014, 2007. 10197
Watanabe, M. and Kimoto, M.: On the persistence of decadal SST anomalies in the North Atlantic, J. Climate, 13, 3017–3028, 2000. 10204
Watson, A. J., Schuster, U., Bakker, D. C. E., Bates, N. R., Corbière, A., González-Dávila, M., Friedrich, T., Hauck, J., Heinze, C., Johannessen, T., Körtzinger, A., Metzl, N., Olafsson, J., Olsen, A., Oschlies, A., Padin, X. A., Pfeil, B., Santana-Casiano, J. M., Steinhoff, T., Telszewski, M., Rios, A. F., Wallace, D. W. R., and Wanninkhof, R.: Tracking the variable North Atlantic sink for atmospheric CO_2, Science, 326, 1391–1393, 2009. 10189, 10190, 10197, 10200
Weiss, R. F.: Carbon dioxide in water and seawater: the solubility of a non-ideal gas, Mar. Chem., 2, 203–215, 1974. 10194, 10198
Weiss, R. F.: Determination of carbon dioxide and methane by dual catalyst flame ionization chromatography and nitrous oxide by electron capture chromatography, J. Chromatogr. Sci., 19, 611–616, 1981. 10191
Zeebe, R. E. and Wolf-Gladrow, D. E.: CO_2 in Seawater: Equilibrium, Kinetics, Isotops, Elsevier Oceanography Series, vol. 65, Elsevier, Amsterdam, The Netherlands, 346 pp., 2001. 10203

BGD
8, 10187–10227, 2011

Table 1. Observed seasonally filtered trends of sea surface temperature (°C yr^{-1}), Salinity (psu yr^{-1}), surface pCO_2 (ppmv yr^{-1}), and sea-air CO_2 fluxes (mol C m^{-2} yr^{-1}) at the NASPG, Northeast Atlantic (NE-Atl.), Caribbean, and BATS stations. The numbers within parentheses represent the associated values from the model simulation.

Parameter	NASPG	NE-Atl.	Caribbean	BATS
Period	Jan 2002–Dec 2007	Jan 2002–Dec 2007	Jan 2002–Dec 2007	Jan 2002–Dec 2007
SST	0.161 (0.047)	0.065 (0.009)	0.074 (0.065)	–0.130 (–0.072)
SSS	0.000 (0.000)	0.008 (0.001)	–0.021 (–0.014)	0.044 (0.004)
pCO_2	–2.630 (1.690)	2.811 (2.542)	1.497 (1.240)	2.853 (0.555)
CO_2 fluxes	–0.284 (0.043)	0.070 (0.101)	–0.035 (–0.030)	0.005 (–0.098)

BGD
8, 10187–10227, 2011

Table 2. Seasonally filtered surface pCO_2 and sea-air CO_2 fluxes trends from the model at the NASPG, Northeast Atlantic, Caribbean, and BATS stations for the 1969–1973 and 1993–1997 periods. Positive trends for the sea-air CO_2 fluxes indicate less uptake, and negative ones indicate more. The atmospheric CO_2 trend is computed from the Mauna Loa data.

Periods	NASPG	NE-Atl.	Caribbean	BATS	atm. CO_2
pCO_2 trend (ppm yr^{-1})					
1969–1973	–0.392	0.449	–0.404	0.965	1.141
1993–1997	2.768	2.834	2.730	0.2396	1.610
CO_2 fluxes trend (moles C m^{-2} yr^{-2})					
1969–1973	–0.110	0.007	–0.075	0.054	
1993–1997	0.255	0.089	0.0336	–0.0582	

BGD
8, 10187–10227, 2011

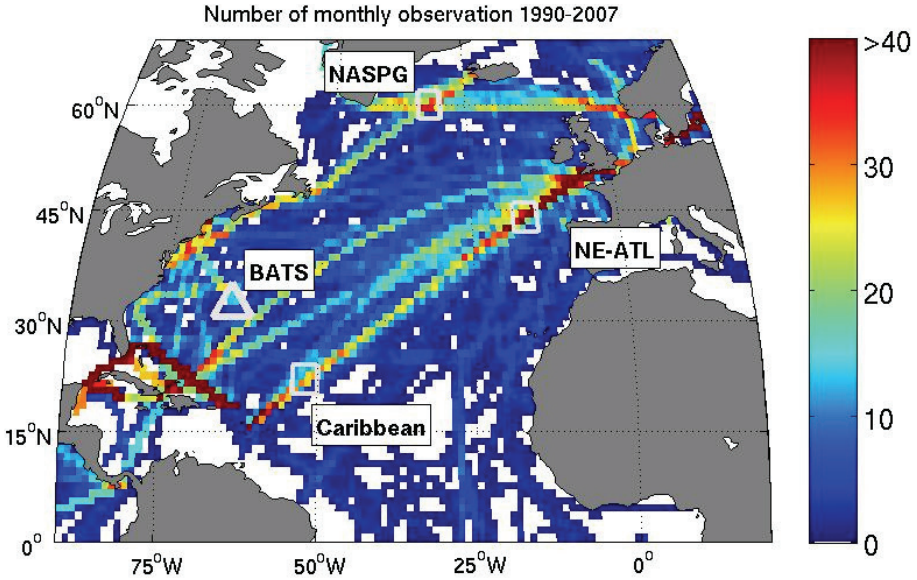

Fig. 1. Map of the total number of monthly underway observation of surface ocean pCO_2 from the SOCAT database binned into one degree boxes. The value (out of a potential 216 monthly observations) is computed based on whether or not any observations are present for the months between 1990 to 2007.

BGD
8, 10187–10227, 2011

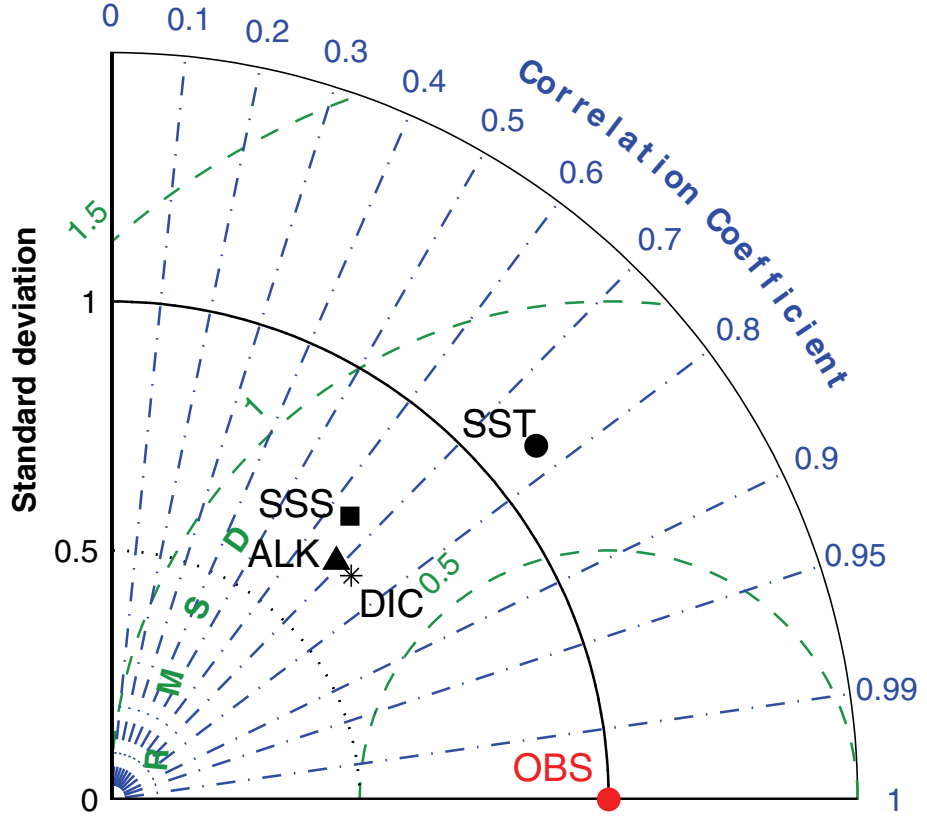

Fig. 2. Taylor diagramme summarizing both the temporal (monthly) and regional (one-degree binned) model-data fit of surface temperature (SST), salinity (SSS), dissolved inorganic carbon (DIC), and alkalinity (ALK). The data are taken from a subset of CARINA database. The standard deviations were normalized to combine the different variables in one diagramme.

BGD
8, 10187–10227, 2011

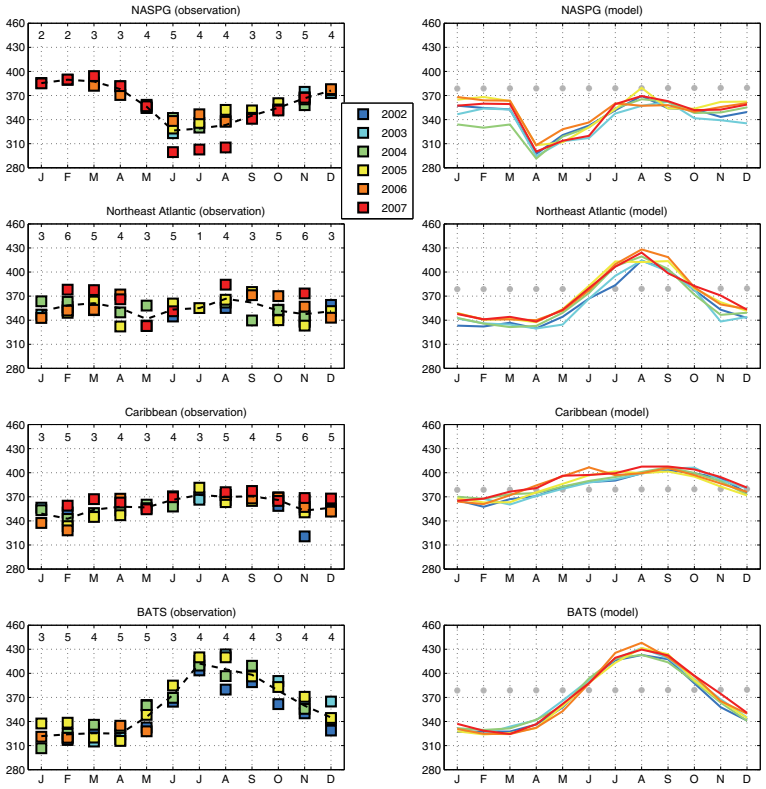

Fig. 3. Observed and simulated seasonal fCO_2 variability (in µatm units) for NASPG, Northeast Atlantic, Caribbean, and BATS for 2002–2007. Dashed black lines in the left panels represent the mean seasonal variation computed from the available observations. Numbers above the left-hand panels give the total number of monthly observations over the 6 yr period. Grey dots in the right hand panels represent the observed monthly mean atmospheric mole fraction in dry air (in ppm units).

BGD
8, 10187–10227, 2011

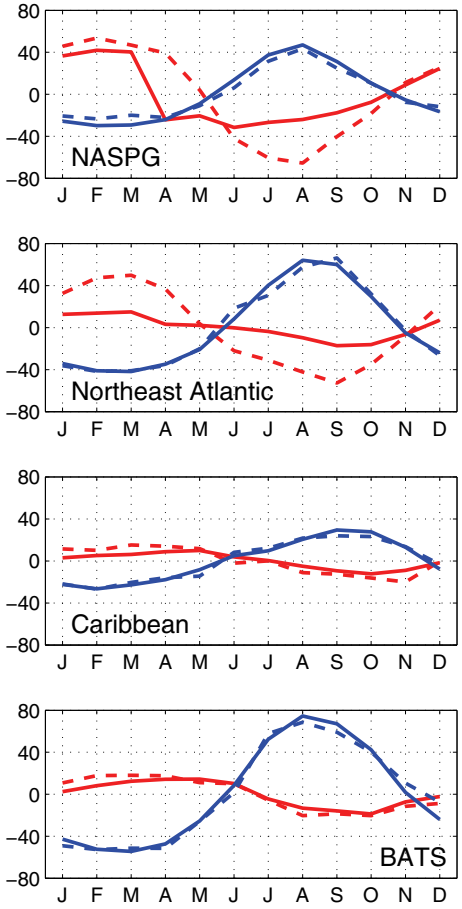

Fig. 4. Comparison of fCO_2-T (blue) and fCO_2-nonT (red) between the model (solid-lines) and the observations (dashed-lines) for different regions in the North Atlantic.

BGD
8, 10187–10227, 2011

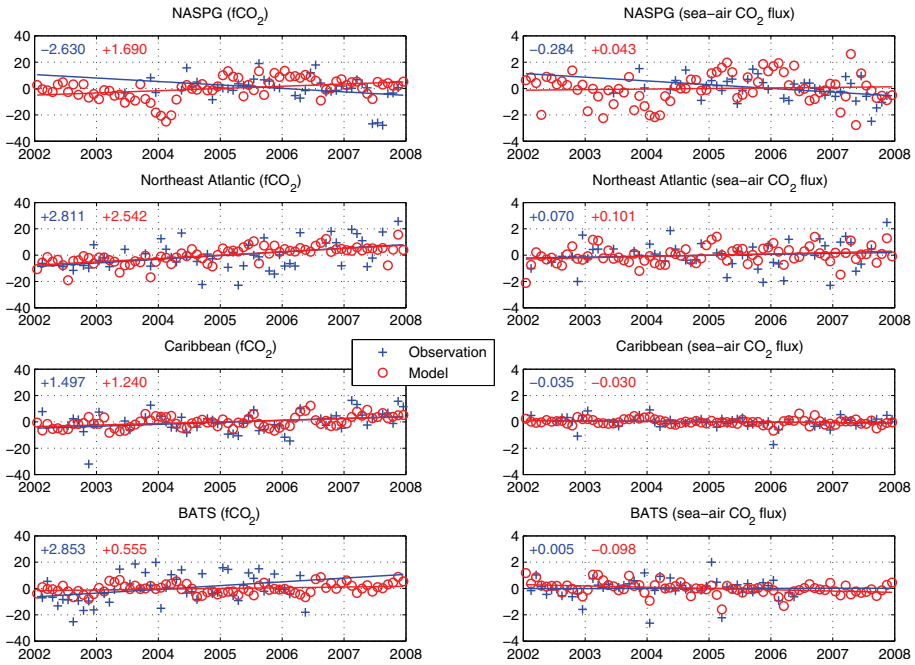

Fig. 5. Observed and simulated seasonally filtered (left-column) surface fCO_2 and (right-column) sea-air CO_2 fluxes at the NASPG, Northeast Atlantic, Caribbean, and BATS stations for 2002–2007. Units are (µatm) and (moles C m^{-2} yr^{-1}), respectively. The coloured numbers represent the annual trend computed after removing the seasonal mean from both observations (blue) and model (red).

BGD
8, 10187–10227, 2011

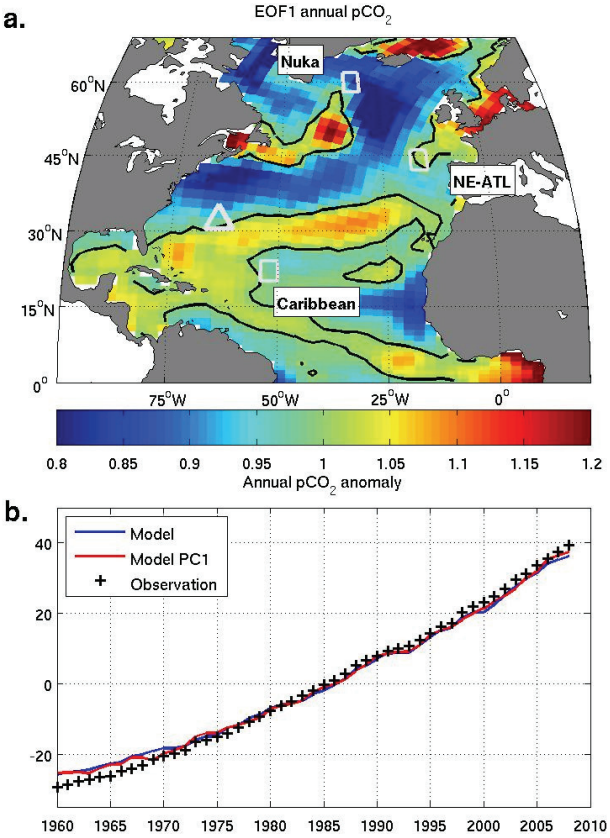

Fig. 6. **(a)** The first empirical orthogonal functions of surface pCO_2 and **(b)** the associated principal component for 1960–2008. The black contour lines in **(a)** indicate the value of one. The temporal variation of PC1 in **(b)** is plotted together with the anomaly of model simulated annual surface pCO_2 (blue line) and annual observed atmospheric CO_2 concentration (black crosses).

BGD
8, 10187–10227, 2011

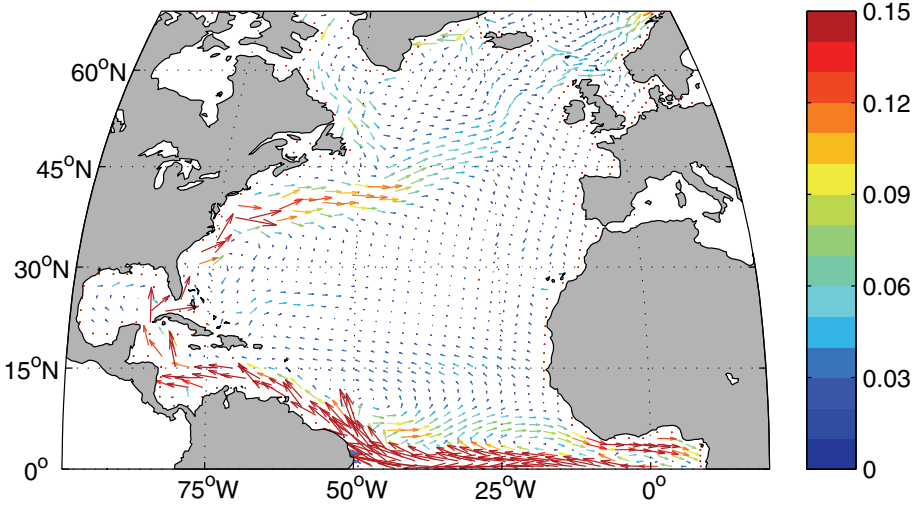

Fig. 7. Simulated mean North Atlantic lateral surface velocity for 1960–2008 ($m\,s^{-1}$).

BGD
8, 10187–10227, 2011

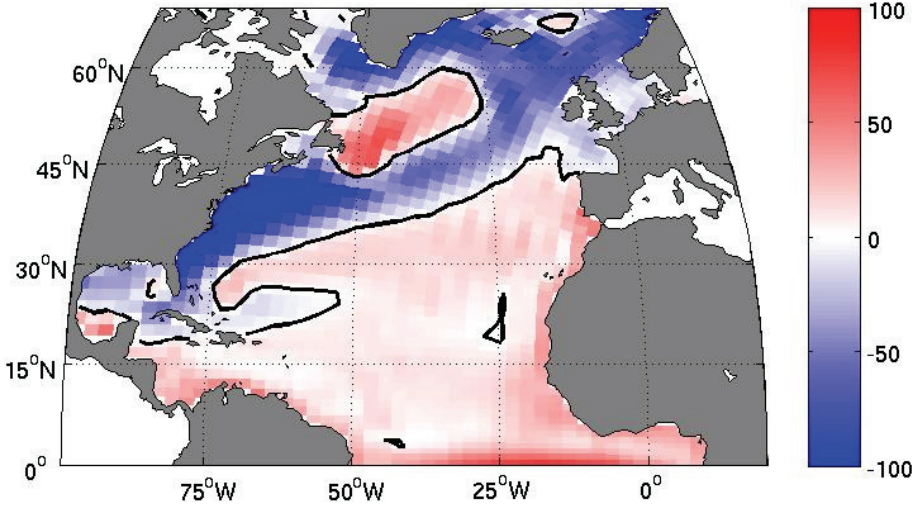

Fig. 8. Simulated mean North Atlantic air–sea heat fluxes for 1960–2008 ($W\,m^{-1}$). The black contour lines indicate the value of zero.

BGD
8, 10187–10227, 2011

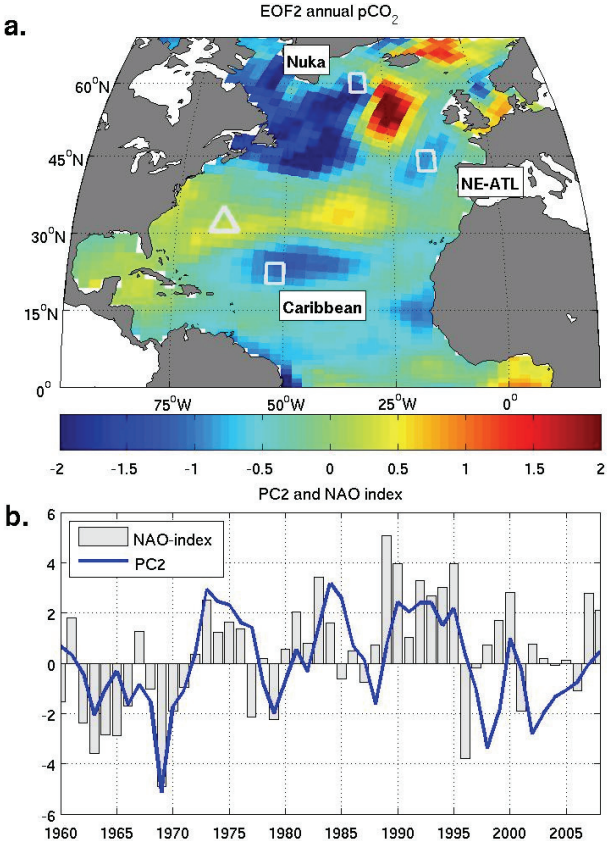

Fig. 9. **(a)** The second empirical orthogonal function of surface pCO_2 and **(b)** the associated principal component (blue line) together with the observed North Atlantic Oscillation index (grey bars) for 1960–2008.

BGD
8, 10187–10227, 2011

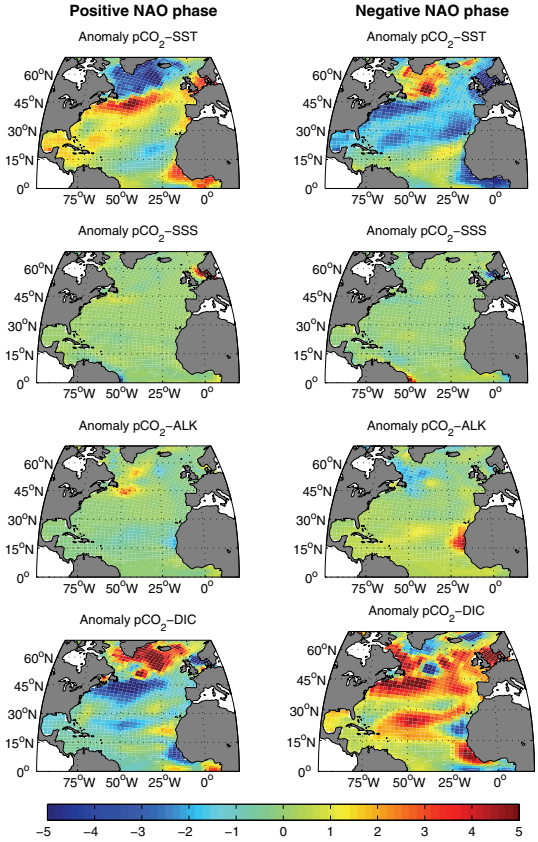

Fig. 10. Composites of anomalies of annual surface pCO_2 associated with changes in surface temperature, salinity, alkalinity, and dissolved inorganic carbon under a dominant positive and negative phase of the North Atlantic Oscillation. Years with dominant positive and negative NAO phases are defined as the year when the winter (December–March) NAO-index is greater and smaller than one standard deviation computed over the period 1960–2008, respectively. Units are in (µatm).

BGD
8, 10187–10227, 2011